

Oxidative Self-Decomposition of the Nickel(III) Complex of Glycylglycyl-L-histidylglycine

Brandon J. Green, Teweldemedhin M. Tesfai, Yi Xie, and Dale W. Margerum*

Department of Chemistry, Purdue University, West Lafayette, Indiana 47907-2084

Received September 3, 2003

Self-decomposition of the nickel(III) doubly deprotonated peptide complex of Gly₂HisGly occurs by base-assisted oxidation of the peptide. At $\leq \text{p}[\text{H}^+] 7.0$, the major pathway is a four-electron oxidation (via 4 Ni(III) complexes) at the α carbon of the N-terminal glycyl residue. The product of this oxidation is oxamylglycylhistidylglycine, which hydrolyzes to yield ammonia and oxalylglycylhistidylglycine. Both of these peptide products decompose to give isocyanatoacetylhistidylglycine. A small amount (2%) of oxidative decarboxylation also is observed. In another major pathway above $\text{p}[\text{H}^+] 7.0$, two Ni(III)–peptide complexes coordinate via an oxo bridge in the axial positions to form a reactive dimer species. This dimer generates two Ni(II)–peptide radical intermediates that cross-link at the α carbons of the N-terminal glycyl residues. In 0.13 mM Ni(III)–peptide at $\text{p}[\text{H}^+] 10.3$, this pathway accounts for 60% of the reaction. The cross-linked peptide is subject to oxidation via atmospheric O₂, where the 2,3-diaminobutanedioic acid is converted to a 2,3-diaminobutenedioic acid. The products observed at $\text{p}[\text{H}^+] < 7.0$ are observed here as well, although in lower yields. The reactivity of Ni^{III}(H₂Gly₂HisGly) is significantly different than that of Cu^{III}(H₂Gly₂HisGly), which undergoes a two-electron oxidation at the histidyl residue with no peptide–peptide cross-linking in basic solution.

Introduction

L-Histidine residues are an important binding site for Ni(II). In human serum albumin, the binding site for nickel is the N-terminal AspAlaHis.¹ Serum albumin is believed to be the primary nickel transport protein in human blood.¹ Additionally, Ni(II) complexes with bound histidine nitrogens are present in at least one nickel-containing enzyme.² Both Ni(II) ions in urease contain two histidine donors.³ Dervan et al.⁴ showed that site-specific DNA cleavage occurred after binding GlyGly-L-His to the amine glycyl terminus of a DNA binding agent and adding Ni(II) with oxidizing agents. We propose that Ni(III) intermediates are present in these reactions. We chose to use Gly₂HisGly because it corresponds to the first four residues of the metal binding site in Dervan's work. The Ni(II) complex of Gly₂HisGly is much more stable than Ni^{II}(H₂GlyGlyHis)[−], which readily oxidizes to Ni(III) in the presence of atmospheric oxygen and decarboxylates.⁵ Ni(III)–peptide complexes containing his-

tidine as the third amino acid residue have been used in site-specific DNA cleavage,^{6–8} RNA cleavage,⁹ protein–protein cross-linking,^{10–12} and protein affinity labeling.¹³ In addition, evidence suggests that superoxide dismutase contains a histidyl nitrogen coordinated to the axial position of a Ni(III) ion.¹⁴ Knowledge of the reaction mechanisms of these species is of interest because of their biochemical importance.

Cu(II/III) complexes that contain a bound L-histidine residue are of similar biological relevance.^{15–17} Previous work

* To whom correspondence should be addressed. E-mail: margerum@purdue.edu.

- (1) Drake, H. L. In *The Bioinorganic Chemistry of Nickel*; Lancaster, J. R. Jr., Ed.; VCH: New York, 1988; pp 112–113.
- (2) Ragsdale, S. W. *Curr. Opin. Chem. Biol.* **1998**, *2*, 208–215.
- (3) Pearson, M. A.; Michel, L. O.; Hausinger, R. P.; Karplus, P. A. *Biochemistry* **1997**, *36*, 8164–8172.
- (4) Mack, D. P.; Dervan, P. B. *J. Am. Chem. Soc.* **1990**, *112*, 4604–4606.

- (5) Bal, W.; Djuran, M. I.; Margerum, D. W.; Gray, E. T., Jr.; Mazid, M. A.; Tom, R. T.; Nieboer, E.; Sadler, P. J. *J. Chem. Soc., Chem. Commun.* **1994**, 1889–1890.
- (6) Liang, Q.; Ananias, D. C.; Long, E. C. *J. Am. Chem. Soc.* **1998**, *120*, 248–257.
- (7) Muller, J. G.; Hickerson, R. P.; Perez, R. J.; Burrows, C. J. *J. Am. Chem. Soc.* **1997**, *119*, 1502–1506.
- (8) Bal, W.; Lukszo, J.; Kasprzak, K. S. *Chem. Res. Toxicol.* **1997**, *10*, 915–921.
- (9) Brittain, I. J.; Xiaofen, H.; Long, E. C. *Biochemistry* **1998**, *37*, 12113–12120.
- (10) Gill, G.; Richter-Rusli, A. A.; Ghosh, M.; Burrows, C. J.; Rokita, S. E. *Chem. Res. Toxicol.* **1997**, *10*, 302–309.
- (11) Brown, K. C.; Yu, Z.; Burlingame, A. L.; Craik, C. S. *Biochemistry* **1998**, *37*, 4397–4406.
- (12) Person, M. D.; Brown, K. C.; Mahrus, S.; Craik, C. S.; Burlingame, A. L. *Protein Sci.* **2001**, *10*, 1549–1562.
- (13) Amini, F.; Kodadek, T.; Brown, K. C. *Angew. Chem., Int. Ed.* **2002**, *41*, 356–359.
- (14) Youn, H.-D.; Youn, H.; Lee, J.-W.; Yim, Y.-L.; Lee, J. K.; Han, Y. C.; Kang, S.-O. *Arch. Biochem. Biophys.* **1996**, *334*, 341–348.

in our research group has shown that trivalent copper tripeptide complexes with histidine as the third amino acid residue undergo oxidative decarboxylation.¹⁵ Regeneration of Cu(III) causes these peptides to give α -hydroxy species, followed by dehydration at the histidyl residue to afford α,β -dehydro peptides. Copper tripeptide complexes with histamine as the third amino acid residue yield only the alkene product, as no terminal carboxyl group is present.¹⁵

Similarly, Ni^{III}(H₂Gly₂His) oxidatively decomposes at the histidyl residue via C-terminal decarboxylation.⁵ Addition of excess oxidant to this Ni(II)-decarboxylated peptide results in an α -hydroxylation at the same residue, and an alkene product forms upon dehydration. The tetrapeptide Cu^{III}-(H₂Gly₂HisGly) complex undergoes oxidation exclusively at the histidyl residue, rather than decarboxylation at the C-terminal carboxyl group.^{16,17}

One purpose of the present work is to determine the site(s) of peptide oxidation in the Ni^{III}(H₂Gly₂HisGly) complex in comparison to the aforementioned work. We find that the main pathway at p[H⁺] 5.4–7.0 is a four-electron oxidation (by 4 Ni(III)) at the N-terminal glycyl α carbon to form oxamylglycylhistidylglycine. At p[H⁺] 8.5–10.3, the Ni(III) complex can exist as an oxo-bridged dimer that undergoes double one-electron oxidations at the N-terminal glycyl α carbons, followed by peptide-peptide cross-linking. The cross-linked product oxidizes in the presence of atmospheric O₂.

Experimental Section

Reagents. All solutions were prepared with doubly deionized, distilled water. NaClO₄ was recrystallized prior to use and standardized gravimetrically. HClO₄ solutions were prepared by purging concentrated (70%) perchloric acid with Ar for 40 min to remove trace oxidants prior to dilution. Ni(ClO₄)₂ solutions were prepared from solid Ni(ClO₄)₂·6H₂O and standardized by EDTA titration with Murexide as the indicator. EDTA was standardized titrimetrically with CaCO₃(s) by using Eriochrome Black T as the indicator. Gly₂-L-HisGly was obtained from Bachem, Inc., and used without further purification. Sodium phosphate and sodium acetate buffers were prepared from their crystalline solids, and the p[H⁺] was adjusted with NaOH, HCl, or HClO₄. Ammonium phosphate, ammonium formate, and ammonium acetate buffers were used in samples for mass spectrometric analysis. The pH was adjusted with ammonia, acetic acid, or formic acid. Oxone (2KHSO₅·K₂SO₄·KHSO₄·5H₂O) was obtained from Aldrich.¹⁸ Standardization of oxone was carried out spectrophotometrically by measuring the absorbance of I₃⁻ at 351 nm¹⁹ formed from the reaction of oxone with excess I⁻ in 50–100 mM [PO₄]_T at pH 2.

Methods. Ni^{II}(H₂Gly₂HisGly)⁻ was prepared by adding the peptide to a solution containing 1 mM Ni(ClO₄)₂, so that the peptide was in 5–10% excess. The solution was adjusted pH 7–7.5 to ensure that the complex was sufficiently formed.

The trivalent metal peptide complexes were prepared by either electrochemical oxidation via a flow-through bulk electrolysis apparatus²⁰ or via chemical oxidation with oxone. Oxidation via the flow-through bulk electrolysis apparatus was carried out at 800–820 mV (vs Ag/AgCl) with a flow rate of 0.43 mL/min. Ni(III) formation via chemical oxidation was carried out by rapid-flow mixing a buffered Ni^{II}(H₂Gly₂HisGly)⁻ solution with a limiting quantity of oxone. In p[H⁺] ranges where the Ni(II) and Ni(III) complexes are unstable (below 6.4 and above 7.0), unbuffered Ni^{II}(H₂Gly₂HisGly)⁻ (pH 7–8) was mixed with oxone, and the resulting Ni(III) solution (pH 6.8–7.5) was immediately collected in a buffered solution. The molar absorptivity of Ni^{III}(H₂Gly₂HisGly) was determined iodometrically in a manner similar to the standardization of oxone.

An Orion 720A digital pH meter and Orion Ross E combination electrodes, stored in solutions of various ionic strengths (0.1, 0.5, and 1.0 M), were used to measure pH values. In cases where the ionic strength was controlled, the pH values were corrected to give $-\log[\text{H}^+]$ (i.e., p[H⁺]) values. An ammonia-sensing ion-selective electrode (Accumet) was used for NH₃ determinations. After acid-catalyzed hydrolysis in the absence of oxygen in 6 M HCl, the sample pH was adjusted to ≥ 12 with NaOH. A CO₂-sensing ion-selective electrode (Accumet) was used for CO₂ determinations after adjusting the solution pH to ≤ 4.5 with NaH₂PO₄ solution. All measurements were carried out at 25.0 °C.

UV–vis spectra were obtained from a Perkin-Elmer Lambda-9 UV–vis–NIR spectrophotometer. An Applied Photophysics stopped-flow spectrophotometer with a cell path of 0.962 cm was used to collect kinetic data. Circular dichroism (CD) spectra were taken with a calibrated Jasco model J600 circular dichroism spectropolarimeter with a 1 cm quartz cell. A Perkin-Elmer Spectrum 2000 FTIR spectrophotometer was used to collect IR data. Frozen EPR spectra were obtained with a Bruker ESP300E spectrometer at a frequency of 9.437 GHz in liquid N₂.

Products of Ni(III)–peptide decomposition were separated by strong cation-exchange chromatography on a Whatman Partisil 10 μm or a Dionex CS-12A strong cation-exchange analytical column (4.6 mm \times 250 mm) on a Varian 5020 liquid chromatograph. Detection was carried out with a Hewlett-Packard 1050 diode array detector.

Samples for electrospray ionization mass spectrometry (ESI-MS), isolated via strong cation-exchange HPLC with a formic acid/ammonium formate eluent, were dried via lyophilization on a VirTis Freezemobile 12 lyophilizer. All ESI-MS analyses were carried out in the Medicinal Chemistry and Molecular Pharmacology Department with a ThermoFinnigan MAT LCQ mass spectrometer system.

Results and Discussion

Characterization of Ni^{II}(H₂Gly₂HisGly)⁻. The Ni^{II}-(H₂Gly₂HisGly)⁻ complex (1 mM and higher) is >99% formed at p[H⁺] 7.0. A stability constant for Ni^{II}(H₂Gly₂HisGly)⁻ (eq 1) was determined spectrophotometrically ($\epsilon = 138 \text{ M}^{-1}\text{cm}^{-1}$ at 424 nm) on the basis of the protonation constants for Gly₂HisGly.¹⁷ A $\log(\beta_{1-21})$ value of $-6.5(7)$ was found, where 1, -2 , and 1 represent to the number of Ni²⁺, H⁺, and Gly₂HisGly species, respectively, involved in the doubly deprotonated complex.¹⁷

$$\beta_{1-21} = \frac{[\text{Ni}^{\text{II}}(\text{H}_2\text{Gly}_2\text{HisGly})^-][\text{H}^+]^2}{[\text{Ni}^{2+}][\text{Gly}_2\text{HisGly}^-]} \quad (1)$$

(15) McDonald, M. R.; Scheper, W. M.; Lee, H. D.; Margerum, D. W. *Inorg. Chem.* **1995**, *34*, 229–237.

(16) McDonald, M. R.; Fredericks, F. C.; Margerum, D. W. *Inorg. Chem.* **1997**, *36*, 3119–3124.

(17) Burke, S. K.; Xu, Y.; Margerum, D. W. *Inorg. Chem.* **2003**, *42*, 5807–5817.

(18) Kennedy, R. J.; Stock, A. M. *J. Org. Chem.* **1960**, *25*, 1901–1906.

(19) Awrey, A. D.; Connick, R. E. *J. Am. Chem. Soc.* **1951**, *73*, 1842–1843.

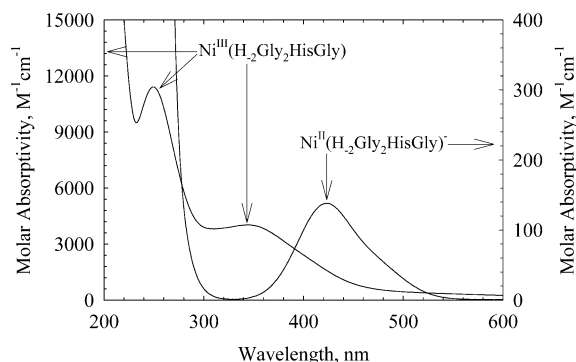


Figure 1. UV-vis spectra of $\text{Ni}^{\text{II}}(\text{H}_{-2}\text{Gly}_2\text{HisGly})^-$ at $\text{p}[\text{H}^+] 7.2$ and $\text{Ni}^{\text{III}}(\text{H}_{-2}\text{Gly}_2\text{HisGly})$ at $\text{p}[\text{H}^+] 2.0$ ($\mu = 0.1 \text{ M}$).

Table 1. Molar Absorptivities for $\text{Ni}^{\text{II}}(\text{H}_{-2}\text{Gly}_2\text{HisGly})^-$ and $\text{Ni}^{\text{III}}(\text{H}_{-2}\text{Gly}_2\text{HisGly})$

| species | λ , nm | ϵ , $\text{M}^{-1} \text{cm}^{-1}$ |
|-------------------------------------------------------------------|----------------|---------------------------------------------|
| $\text{Ni}^{\text{II}}(\text{H}_{-2}\text{Gly}_2\text{HisGly})^-$ | 424 | 138(1) |
| $\text{Ni}^{\text{III}}(\text{H}_{-2}\text{Gly}_2\text{HisGly})$ | 247 | $1.16(1) \times 10^4$ |
| $\text{Ni}^{\text{III}}(\text{H}_{-2}\text{Gly}_2\text{HisGly})$ | 343 | $4.02(3) \times 10^3$ |

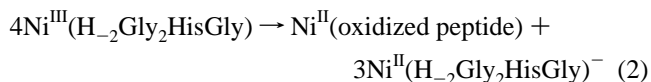
Preparation of $\text{Ni}^{\text{III}}(\text{H}_{-2}\text{Gly}_2\text{HisGly})$. In some cases, the flow-through bulk electrolysis cell was used to generate $\text{Ni}^{\text{III}}(\text{H}_{-2}\text{Gly}_2\text{HisGly})$ at pH 7.5–8. Electrolysis of the unbuffered solution lowers the pH to 2–5 and decreases the amount of doubly deprotonated Ni(II) complex available for oxidation. However, the lowered pH of the electrolyzed solution stabilizes the Ni(III) complex, as opposed to higher pH (>7.5) which causes rapid decomposition of Ni(III). Therefore, yields of $\text{Ni}^{\text{III}}(\text{H}_{-2}\text{Gly}_2\text{HisGly})$ were variable from 10 to 75%. The electrolysis products were immediately collected into appropriate buffer solutions. Quantitation of Ni(III) was achieved by collecting the species in a solution of 0.01 M HClO_4 and measuring the resulting absorbance at 343 nm. At this pH, the $\text{Ni}^{\text{III}}(\text{H}_{-2}\text{Gly}_2\text{HisGly})$ complex has a half-life of approximately 12 h, and oxidative self-decomposition during the collection process is negligible.

Oxone and magnesium monoperoxyphthalate have both been used to activate Ni(II)– Gly_2His complexes linked to proteins in site-specific DNA cleavage^{4,6} and protein–protein cross-linking.^{10–12} It has been postulated that Ni(III) intermediates were present.^{6,10} Our stopped-flow kinetic data show that $\text{Ni}^{\text{III}}(\text{H}_{-2}\text{Gly}_2\text{HisGly})$ can be formed in 99+% yield with oxone at $\text{p}[\text{H}^+] 6.7$ (Figures S1 and S2 in the Supporting Information). Due to the relatively short half-life of $\text{Ni}^{\text{III}}(\text{H}_{-2}\text{Gly}_2\text{HisGly})$ at neutral and basic pH (minutes to milliseconds, respectively), oxone provides an effective route to generating Ni(III) without the need for additional spectrophotometric quantitation.

Characterization of $\text{Ni}^{\text{III}}(\text{H}_{-2}\text{Gly}_2\text{HisGly})$. The UV-vis spectrum of $\text{Ni}^{\text{III}}(\text{H}_{-2}\text{Gly}_2\text{HisGly})$ exhibits strong ligand-to-metal charge-transfer bands at 247 and 343 nm. UV-vis spectral bands of the di- and trivalent Ni complexes are shown in Figure 1, and their molar absorptivities are summarized in Table 1.

A frozen EPR spectrum in liquid N_2 and pH 0.7 exhibits signals at 2980 G ($g_{\perp} = 2.25$) and 3330 G ($g_{\parallel} = 2.02$, Figure S3). These g values are in agreement with those reported for other Ni(III)–peptide complexes.^{5,21,22}

Decomposition Reactions from $\text{p}[\text{H}^+] 5.4$ –7.0. The predominant pathway for oxidative self-decomposition is a four-electron oxidation at the α carbon of the N-terminal glycyl residue. In this oxidation, 4 mol of $\text{Ni}^{\text{III}}(\text{H}_{-2}\text{Gly}_2\text{HisGly})$ react to form 1 mol of oxidized peptide, with a recovery of 3 mol of $\text{Ni}^{\text{II}}(\text{H}_{-2}\text{Gly}_2\text{HisGly})$ (eq 2).



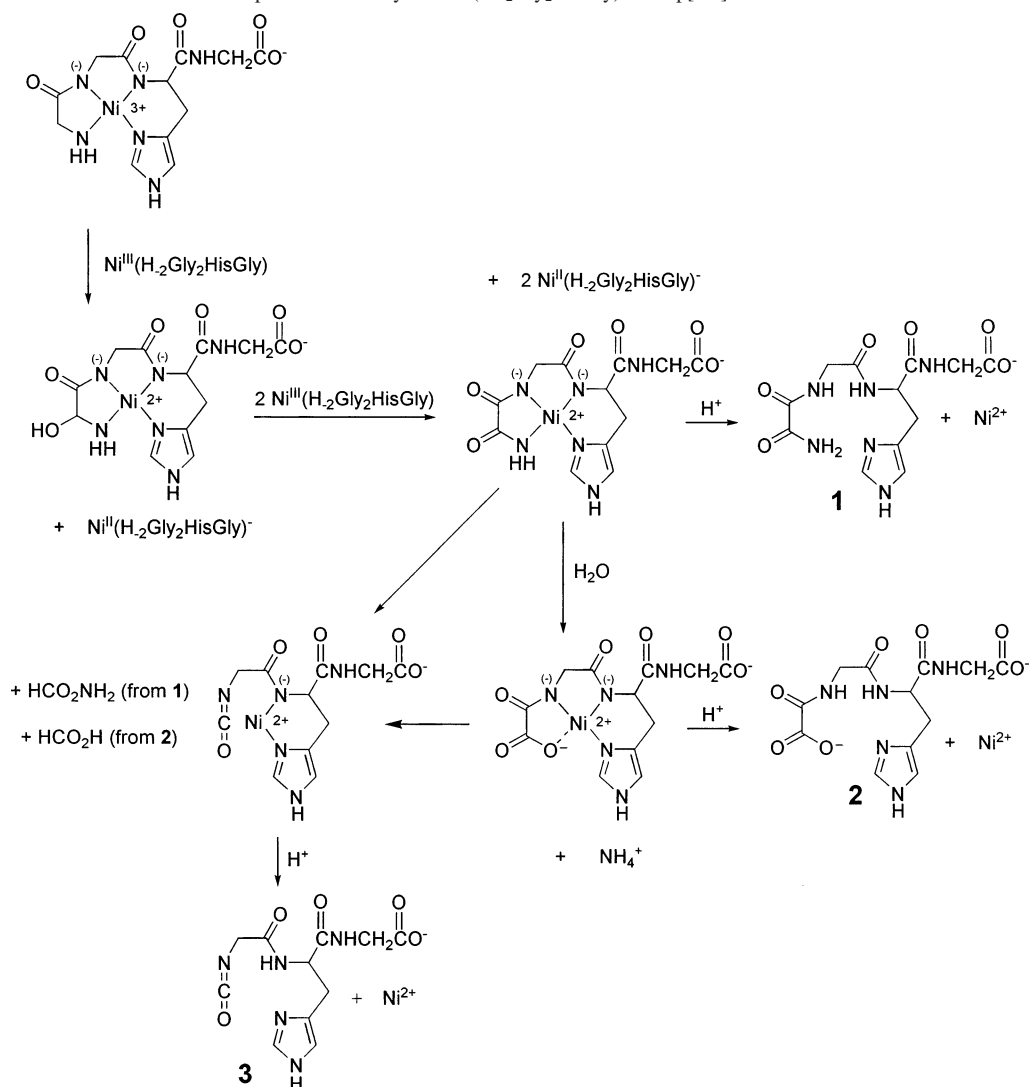
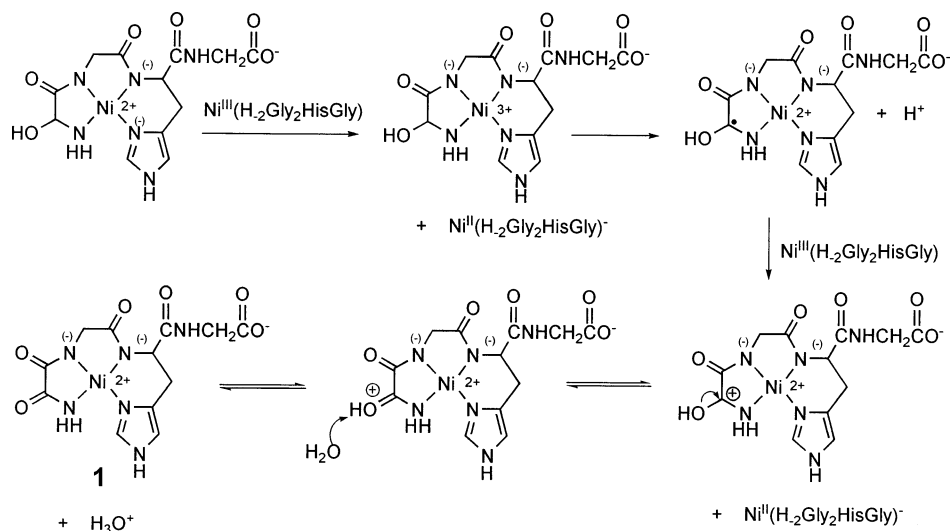
A peptide recovery of 72(2)% at $\text{p}[\text{H}^+] 6.7$ was obtained, which approximates the stoichiometry in eq 2. As will be shown, chromatographic and ESI-MS data identify the product of this reaction as oxamylglycylhistidylglycine (**1**, Scheme 1). This product can hydrolyze to oxalylglycylhistidylglycine (**2**) or decay to isocyanatoacetylhistidylglycine (**3**) and formamide. It is also possible that product **2** decays to the isocyanatopeptide (**3**) and formic acid. Hydrolytic release of NH_3 from oxamylglycylhistidylglycine and formamide (Scheme 1) is supported by an ammonia recovery of 18(1)% of the total Ni(III) present. Taking the reaction stoichiometry (eq 2) into consideration, the ammonia release accounts for at least 72(4)% of the total possible reaction. In addition to this pathway, a two-electron decarboxylation at the C-terminal glycyl residue was also observed (2(1)% at $\text{p}[\text{H}^+] 6.4$).

The reaction at the N-terminal glycyl residue consists of a two-electron oxidation in which 2 mol of the $\text{Ni}^{\text{III}}(\text{H}_{-2}\text{Gly}_2\text{HisGly})$ form 1 mol of $\text{Ni}^{\text{II}}(\text{H}_{-2}(\alpha\text{-OH-Gly})\text{GlyHisGly})^-$ and 1 mol of $\text{Ni}^{\text{II}}(\text{H}_{-2}\text{Gly}_2\text{HisGly})^-$ (Scheme 1). $\text{Ni}^{\text{II}}(\text{H}_{-2}(\alpha\text{-OH-Gly})\text{GlyHisGly})^-$ rapidly reacts with an additional 2 mol of $\text{Ni}^{\text{III}}(\text{H}_{-2}\text{Gly}_2\text{HisGly})$ to form $\text{Ni}^{\text{II}}(\text{H}_{-2}\text{oxamylglycylhistidylglycine})^-$ (**1**) and 2 mol of $\text{Ni}^{\text{II}}(\text{H}_{-2}\text{Gly}_2\text{HisGly})^-$. The proposed oxidation of $\text{Ni}^{\text{II}}(\text{H}_{-2}(\alpha\text{-OH-Gly})\text{GlyHisGly})^-$ consists of two successive rapid electron-transfer reactions. A possible mechanism is shown in Scheme 2, where the $\text{Ni}^{\text{II}}(\text{H}_{-2}(\alpha\text{-OH-Gly})\text{GlyHisGly})^-$ intermediate is reoxidized to Ni(III), which oxidizes the ligand to a radical form of $\text{Ni}^{\text{II}}(\text{H}_{-2}(\alpha\text{-OH-Gly})\text{GlyHisGly})^-$. This radical can then reduce another Ni(III) complex to afford a Ni(II) complex and a carbocation intermediate that reacts further to give **1**. We propose that $\text{Ni}^{\text{II}}(\text{H}_{-2}(\alpha\text{-OH-Gly})\text{GlyHisGly})^-$ is sufficiently long-lived to undergo additional oxidation to Ni(III). Stopped-flow kinetic data show that even at $\text{p}[\text{H}^+] 5.4$, where $\text{Ni}^{\text{II}}(\text{H}_{-2}\text{Gly}_2\text{HisGly})^-$ can dissociate, the rate of dissociation is not rapid ($k = 4.07(1) \times 10^{-3} \text{ s}^{-1}$). Hence we propose that the $\text{Ni}^{\text{II}}(\text{H}_{-2}(\alpha\text{-OH-Gly})\text{GlyHisGly})^-$ intermediate is sufficiently stable to reoxidize to Ni(III) via rapid electron-transfer reactions. Although the steps shown in Scheme 2

(20) Neubecker, T. A.; Kriksey, S. T.; Chellappa, K. L.; Margerum, D. W. *Inorg. Chem.* **1979**, *18*, 444–448.

(21) Lappin, A. G.; Murray, C. K.; Margerum, D. W. *Inorg. Chem.* **1978**, *17*, 1630–1634.

(22) Pappenhagen, T. L.; Kennedy, W. R.; Bowers, C. P.; Margerum, D. W. *Inorg. Chem.* **1985**, *24*, 4356–4362.

Scheme 1. Four-Electron Oxidative Decomposition Pathway of Ni^{III}(H₂Gly₂HisGly) from p[H⁺] 5.4–7.0**Scheme 2.** Possible Detailed Mechanism for the Four-Electron Oxidation to Give **1**

are not observed kinetically, products **1–3** have been characterized.

Identification of Products from p[H⁺] 5.4–7.0. ESI-MS data of Ni(III)–peptide decomposition products at pH

7.2 (Figure 2) show the [M + H]⁺ adducts of the oxamyl- and oxalylglycylhistidylglycine products (*m/z* 341 and 342, respectively). MS-MS data of the *m/z* 341 and *m/z* 342 peaks show species that correspond to the loss of neutral molecules,

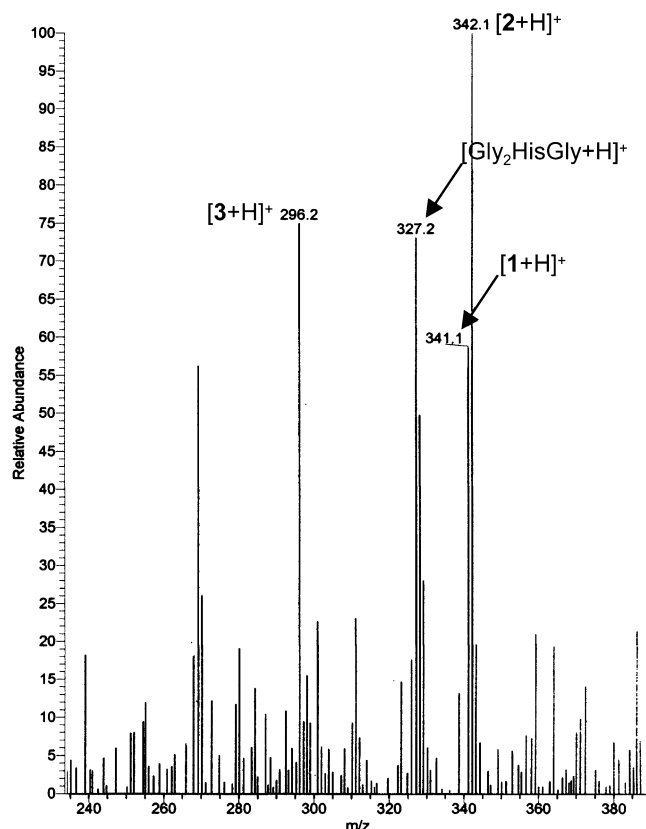


Figure 2. ESI-MS of 0.5 mM $\text{Ni}^{\text{III}}(\text{H}_2\text{Gly}_2\text{HisGly})$ decomposition products originally at pH 7.2. Oxamylglycylhistidylglycine (**1**), oxalylglycylhistidylglycine (**2**), isocyanatoacetylhistidylglycine (**3**), and unreacted $\text{Gly}_2\text{HisGly}$ are present.

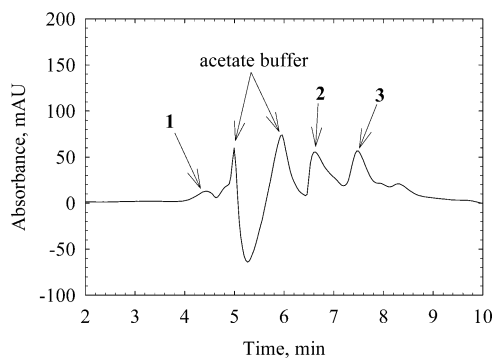


Figure 3. Chromatographic separation of the decomposition products of 0.25 mM $\text{Ni}^{\text{III}}(\text{H}_2\text{Gly}_2\text{HisGly})$ (originally in 20 mM $[\text{OAc}]_{\text{T}}$ at pH 5.8). The sample pH was adjusted to 4.4 with formic acid prior to injection. Chromatographic conditions: Strong cation-exchange separation in 25 mM $[\text{formate}]_{\text{T}}$ (pH 4.4) at 0.5 mL/min up to 9 min with a linear gradient to 2.0 mL/min at 10.0 min, 100 μL injection, and $\lambda_{\text{det}} = 225$ nm. Oxamylglycylhistidylglycine (**1**), oxalylglycylhistidylglycine (**2**), isocyanatoacetylhistidylglycine (**3**), and acetate buffer were identified via ESI-MS. The acetate buffer peak is distorted because it coelutes with the injection peak.

such as H_2O , CO_2 , and glycine (Tables S1 and S2, respectively). These data indicate that the m/z 341 and 342 species are oxidized peptide products. A chromatogram of $\text{Ni}^{\text{III}}(\text{H}_2\text{Gly}_2\text{HisGly})$ self-decomposition products is shown in Figure 3, where oxalylglycylhistidylglycine (**2**) and oxamylglycylhistidylglycine (**1**) were identified from mass spectrometric analysis. The reaction products in Figure 3 have relatively low retention times. This is due to the replacement of the N-terminal amino group with a nonbasic amide group via

Table 2. $\text{Gly}_2\text{HisGly}$ Recoveries from $\text{Ni}^{\text{III}}(\text{H}_2\text{Gly}_2\text{HisGly})$

| atmospheric conditions | $\text{p}[\text{H}^+]$ ($\mu = 0.1$ M) | % $\text{Gly}_2\text{HisGly}$ recovery |
|------------------------|-----------------------------------------|----------------------------------------|
| air-saturated | 5.4 | 79(2) |
| air-saturated | 6.7 | 72(2) |
| argon-saturated | 6.7 | 80(2) |
| air-saturated | 9.2 ^a | 48(2) |
| air-saturated | 10.3 ^a | 30(2) |

^a $\mu = 1.0$ M, $[\text{Ni}^{\text{III}}(\text{H}_2\text{Gly}_2\text{HisGly})] = 0.127$ mM.

the four-electron oxidation. Such a retention time would not be expected for $(\alpha\text{-OH-Gly})\text{GlyHisGly}$, in agreement with our proposed four-electron oxidation. Additionally, recent work has shown that $(\alpha\text{-OH-Gly})\text{GlyHistamine}$, which is similar in structure to $(\alpha\text{-OH-Gly})\text{GlyHisGly}$, is not a stable species.²³ Oxalylglycylhistidylglycine (**2**) exhibits a series of absorbance bands that extend well into the visible range (Figure S5). Oxamic acid also exhibits an absorbance that extends up to 300 nm.

Isocyanatoacetylhistidylglycine (**3**) was consistently observed as a product of $\text{Ni}^{\text{III}}(\text{H}_2\text{Gly}_2\text{HisGly})$ decomposition from $\text{p}[\text{H}^+]$ 5.4 to 7.0. Mass spectrometric and chromatographic data (Figures 2 and 3, respectively) show that this species is formed in appreciable amount. In addition, MS-MS data of the m/z 296 molecular ion show an intense $[3 + \text{H} - \text{Gly}]^+$ fragment at m/z 221 (Table S3). An IR spectrum of $\text{Ni}^{\text{III}}(\text{H}_2\text{Gly}_2\text{HisGly})$ products shows bands at 2050 and 2210 cm^{-1} that we attribute to an isocyanate group. However, the mechanism for isocyanate formation is not well understood. It is possible that **3** is formed from the decay of **1** and/or **2** (Scheme 1). Isocyanates have been observed as products of metal-catalyzed protein oxidation where oxygen is present.^{24,25} In these cases, atmospheric O_2 inserts into an α carbon radical to form a peroxy peptide intermediate, which further reacts to form an isocyanato peptide. However, in our work, atmospheric O_2 does not play a role in isocyanate formation. If O_2 were to react with oxidized peptide intermediates, the resulting peroxy peptide could oxidize additional $\text{Ni}^{\text{II}}(\text{H}_2\text{Gly}_2\text{HisGly})^-$. This would result in significantly different peptide recoveries. However, $\text{Gly}_2\text{HisGly}$ recoveries from its trivalent complex at $\text{p}[\text{H}^+]$ 6.7 in the presence and absence of atmospheric O_2 were 72(2)% and 80(2)%, respectively (Table 2). The observed peptide recoveries do not support an oxygen-mediated pathway. Additionally, the O_2 insertion into $\text{Ni}(\text{II})$ -peptide radical intermediates would affect the observed rate constants of $\text{Ni}(\text{III})$ loss. Kinetic studies of $\text{Ni}(\text{III})$ decay in the presence and absence of oxygen show no significant deviation in the rate of $\text{Ni}(\text{III})$ loss. Isocyanate formation via photolysis of $\text{Cu}(\text{III})$ -peptide complexes has been reported.^{26,27} However, it is doubtful that photochemistry plays a role in our work.

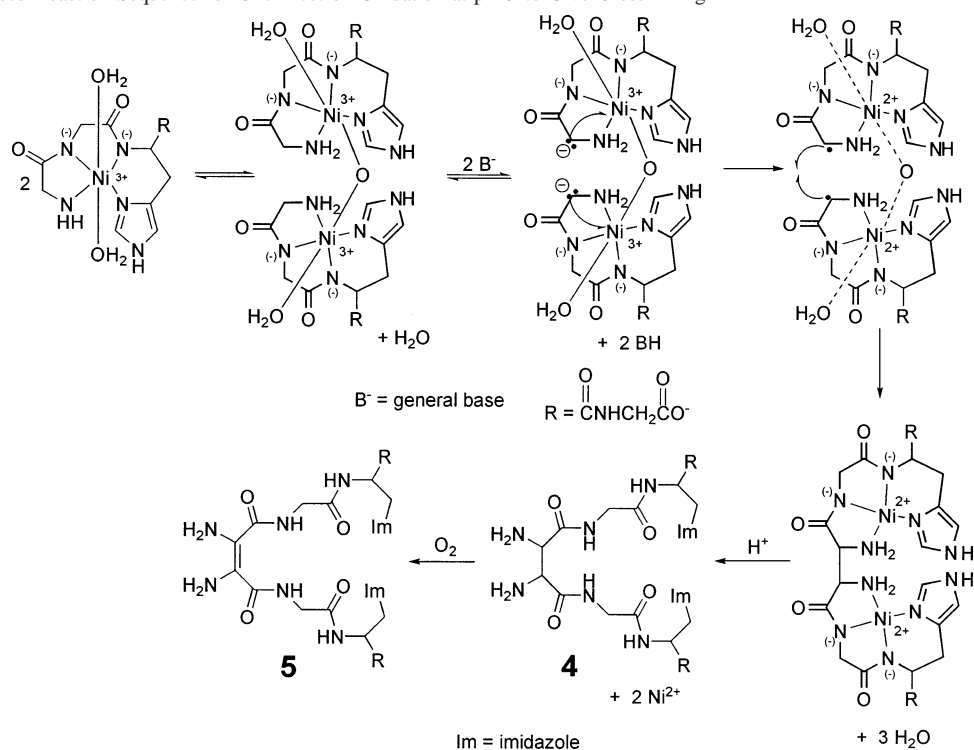
(23) Green, B. J.; Tesfai, T. M.; Margerum, D. W. To be submitted for publication.

(24) Berlett, B. S.; Stadtman, E. R. *J. Biol. Chem.* **1997**, *272*, 20313–20316.

(25) Stadtman, E. R.; Berlett, B. S. *Chem. Res. Toxicol.* **1997**, *10*, 485–494.

(26) Hamburg, A. W.; Margerum, D. W. *Inorg. Chem.* **1983**, *22*, 3884–3893.

(27) Hinton, J. P.; Margerum, D. W. *Inorg. Chem.* **1986**, *25*, 3248–3256.

Scheme 3. Proposed Reaction Sequence for One-Electron Oxidation at pH 9 to Give Crosslinking^a

^a After acidification, species **4** and **5** are isolated.

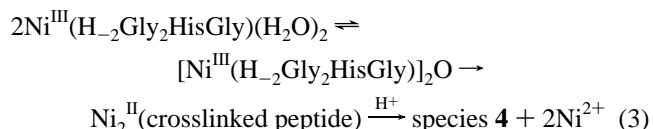
Isocyanate formation was found when the Ni(III) complex was generated under infrared light and allowed to decompose in the absence of light.

Comparison of Products from Ni(III) and Cu(III) Complexes of Gly₂HisGly. Ni^{III}(H₂Gly₂HisGly) reacts much differently than Cu^{III}(H₂Gly₂His) and Ni^{III}(H₂Gly₂His) with regard to C-terminal decarboxylation. Decarboxylation yields from Ni^{III}(H₂Gly₂HisGly) (2% of the total possible reaction) are much lower than the latter two species (100%).^{5,15} In general, it appears that the coordination of a C-terminal carboxylate group to the axial site of a trivalent metal, followed by oxidation via the trivalent metal, is less favorable than oxidation at the α carbon of an amino acid residue. This assumption is corroborated by the fact that Cu^{III}(H₂Gly₂HisGly) undergoes oxidation at the histidyl α carbon with no decarboxylation.^{16,17} Decarboxylations of the tripeptide Cu^{III}(H₂Gly₂His) and Ni^{III}(H₂Gly₂His) complexes do not occur via direct contact of the carboxylate group with the trivalent metal.

The comparison of the reactivity of Ni^{III}(H₂Gly₂HisGly) with its Cu(III) analogue introduces another interesting point. The main pathway of Cu^{III}(H₂Gly₂HisGly) decomposition is proton abstraction at the α carbon of the histidyl residue followed by a two-electron oxidation to form Gly₂(α -OH-His)Gly. This species then dehydrates to form the alkene peptide Gly₂(α,β -dehydro-His)Gly.^{16,17} However, chromatographic, mass spectrometric, and UV-vis data show no evidence of the formation of this Gly₂(α,β -dehydro-His)Gly product from Ni^{III}(H₂Gly₂HisGly). Additionally, a circular dichroism study of Ni^{III}(H₂Gly₂HisGly)⁻ and the decomposition products of Ni^{III}(H₂Gly₂HisGly) at p[H⁺] 7.3 gave very similar spectra. The molar ellipticities were 30.70

mdeg and 30.68 mdeg, respectively, lending further evidence that the stereogenic α carbon at the histidyl residue is not lost due to alkene formation. The reason for the different sites of ligand oxidation for the Ni(III) compared to the Cu(III) species is not well understood. However, Cu(III)-peptide complexes can have deprotonated amine groups^{15,16,20} with multiple bonding to the metal.²⁰ These complexes are not oxidized at the N-terminal glycol groups. On the other hand, Ni(III)-peptide complexes do not form stable species by amine deprotonation.^{28,29} The present work shows that they are oxidized at the N-terminal glycol residue. In addition, the first-order decomposition of Cu^{III}(H₂Gly₂HisGly) is approximately 7 times faster than Ni^{III}(H₂Gly₂HisGly) at p[H⁺] 6.6.¹⁷

Decomposition Reactions from p[H⁺] 8.5 to 10.3. The decomposition kinetics of Ni^{III}(H₂Gly₂HisGly) changes from first- to second-order above p[H⁺] 8.5.³⁰ The reaction undergoes an additional pathway in basic solution, where two Ni(III)-peptide complexes can form an oxo-bridged dimer species.³⁰ We propose that an oxo-bridged dimer forms via axial coordination with two Ni(III) complexes. Each peptide undergoes a one-electron oxidation. The resulting radicals then recombine at their α carbons to give a cross-linked peptide. The reaction is outlined in Scheme 3 and eq 3.



Chromatographic, mass spectrometric, and spectroscopic data show that the 2,3-diaminobutanedioc acid product (**4**)

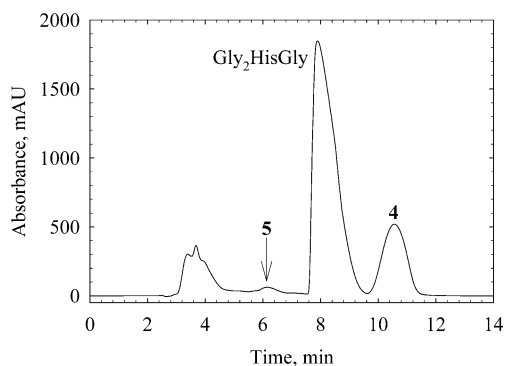


Figure 4. Chromatographic separation of 0.25 mM Ni^{III}(H₂Gly₂HisGly) products originally at pH 9.0 in 20 mM [CO₃]_T. The cross-linked Gly₂-HisGly product (**4**) and its oxidation product (**5**) are present. Sample pH adjusted to 4.4 with formic acid prior to injection. Chromatographic conditions: Strong cation-exchange separation in 25 mM [formate]_T (pH 4.40) at 1.0 mL/min, 500 μL injection, and λ_{det} = 225 nm.

slowly oxidizes in the presence of atmospheric O₂ at pH 4 to yield a 2,3-diaminobutenedioic acid product (**5**, Scheme 3). Recoveries of Gly₂HisGly from its Ni(III) complex are significantly lower at p[H⁺] 8.5–10.3 than at p[H⁺] 5.4–7. At p[H⁺] 10.3, the major pathway of Ni(III) decomposition is the one-electron oxidation pathway to give the cross-linked peptide. The four-electron oxidation pathway (Scheme 1, eq 2) also occurs at p[H⁺] 8.5–10.3.

Ni(III) complexes have been shown to link axially via oxo bridges.^{30,31} A bent geometry of the oxo bridge is proposed that gives close proximity of the peptides and their carbon radical intermediates. Above p[H⁺] 10.3, most of the reaction proceeds via radical recombination to give a cross-linked peptide product with a new C–C bond.

Identification of Species 4. The chromatogram in Figure 4 shows a product (**4**) that elutes 2.7 min later than Gly₂-HisGly. ESI-MS data of **4** show a [4 + H]⁺ adduct at *m/z* 651 (Figure 5) and a [4 + 2H]²⁺ adduct at *m/z* 326 (not shown). This species (MW = 650) corresponds to the cross-linked peptide with a molecular weight that is two mass units less than twice the mass of the parent peptide (MW = 326). MS-MS analysis of the *m/z* 651 peak shows the loss of neutral molecules, along with a [Gly₂HisGly + H]⁺ fragment at *m/z* 327 (Table S4). The identification of the [4 + 2H]²⁺ species is supported by MS-MS fragments of [4 + 2H – Gly]²⁺ and [4 + 2H – H₂O]²⁺ at *m/z* 288.6 and 317, respectively (Table S5). Supporting evidence for the regiochemistry of peptide–peptide cross-linking will be discussed later.

The peptide–peptide cross-linking becomes more significant as pH increases (Tables 2 and 3). If the four-electron (Scheme 1) and the double one-electron oxidation (Scheme 3) pathways are the only ones that occur, the percentage of each pathway at a particular p[H⁺] can be determined by measuring the amount of Gly₂HisGly recovered. The four-electron pathway will give a 75% Gly₂HisGly recovery (eq

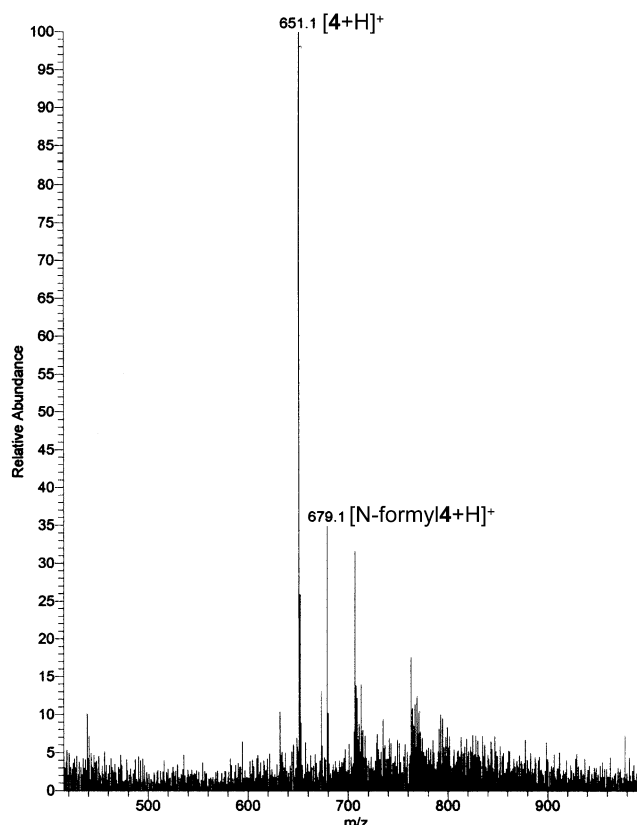


Figure 5. ESI-MS of cross-linked Gly₂HisGly product **4** from Figure 4. A [4 + 2H]²⁺ adduct at *m/z* 326 (not shown) is also present.

Table 3. Pathway Selectivity of Ni^{III}(H₂Gly₂HisGly) Decomposition vs p[H⁺]^a

| p[H ⁺] | % rxn with 4 e ⁻ oxid | % rxn with double 1 e ⁻ oxid |
|--------------------|----------------------------------|-----------------------------------------|
| 6.7 ^b | 96(4) | 4(4) |
| 9.2 ^c | 64(3) | 36(3) |
| 10.3 ^c | 40(3) | 60(3) |

^a The percent of reaction following the four-electron oxidation path is calculated by dividing the percent Gly₂HisGly recovery by 75%. The remaining percentage follows the double one-electron pathway. ^b μ = 0.1 M. ^c μ = 1.0 M, [Ni^{III}(H₂Gly₂HisGly)] = 0.127 mM.

2), and the double one-electron pathway will give a 0% Gly₂-HisGly recovery (eq 3). Therefore, the fraction of the reaction following the four-electron pathway is the peptide recovery divided by 75%. As shown in Table 3, the reaction follows the four-electron decomposition path at p[H⁺] 6.7. However, as the p[H⁺] is increased, the equilibrium of the reaction shifts more toward the double one-electron pathway.³⁰ In fact, the one-electron pathway is the major one at p[H⁺] 10.3 and 0.127 mM Ni(III), accounting for 60(3)% of the reaction. The peptide–peptide cross-linking observed with Ni(III) is not observed in the Cu(III) analogue,^{16,17} as the square planar geometry of Cu(III) precludes the formation of an oxo bridge between two Cu(III) species.

Identification of Species 5. An ESI mass spectrum of the 2,3-diaminobutenedioic acid product (species **5**) is shown in Figure S9. MS-MS data of the *m/z* 649 molecular ion and the *m/z* 325 [5 + 2H]²⁺ adduct are shown in Tables S6 and S7, respectively. Species **5** is formed by atmospheric O₂ oxidation of **4**. The 2,3-diaminobutenedioic acid forms in a

(28) Kirvan, G. E.; Margerum, D. W. *Inorg. Chem.* **1985**, *24*, 3245–3253.

(29) Tesfai, T. M. M.S. Thesis, Purdue University, May 2003.

(30) Tesfai, T. M.; Green, B. J.; Margerum, D. W. To be submitted for publication.

(31) Bag, B.; Mondal, N.; Rosair, G.; Mitra, S. *Chem. Commun.* **2000**, 1729–1730.

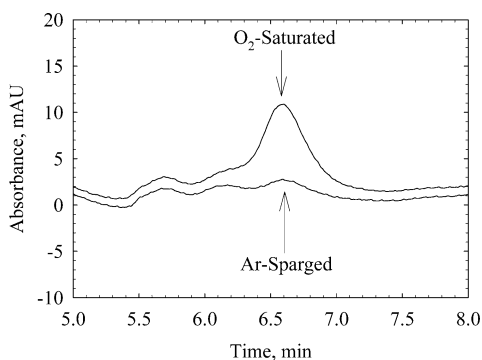


Figure 6. Chromatogram containing the oxidized cross-linked Gly₂HisGly product (**5**) held for 3 h at p[H⁺] 4.0 under O₂-rich and O₂-free conditions. Chromatographic conditions: Strong cation-exchange separation in 25 mM [formate]_T (pH 4.40) at 1.0 mL/min, 100 μL injection, and λ_{det} = 225 nm. The unreacted Gly₂HisGly and other oxidized peptide products are omitted for clarity.

6-fold greater yield when the reaction is acidified to p[H⁺] 4.0 and saturated with O₂ for 3 h than when the products are sparged with Ar under the same conditions (Figure 6). It is unlikely that Ni(II) is involved in this oxidation, as strong σ donors are needed to stabilize the Ni(III) species that would oxidize the ligand. The doubly deprotonated Ni(II)–peptide complex is needed for Ni(III) formation, and it is not formed at p[H⁺] 4.0. Three conjugated double bonds help to stabilize species **5**. The lone pair electrons from the enamine nitrogens can participate with the C=C double bond and adjacent carbonyl groups to provide additional stability via resonance forms. MS-MS data of **4** show that the cross-linking C–C bond breaks readily in the gas phase. The strong (100% relative abundance) peak at *m/z* 327 from the MS-MS spectrum of [**4** + H]⁺ correlates to a [Gly₂HisGly + H]⁺ adduct (Table S4). This indicates that a gas phase rearrangement involving the cross-linked α carbons has occurred. These data suggest that the cross-linking C–C bond in **4** is relatively weak. However, the MS-MS spectrum of [**5** + H]⁺ does not show a similar adduct (Table S6). The lack of this type of rearrangement in **5** is consistent with the presence of stronger bonding (a double bond) between the α carbons. Furthermore, the UV–vis spectrum of **5** has a strong band with a λ_{max} of 275 nm. Such an absorbance can be attributed to electron delocalization between the enamino C=C bond and the two adjacent carbonyl groups. The unpaired electrons from the enamino nitrogens may also contribute to this absorbance.

Regiochemistry of Peptide–Peptide Cross-Linking. For several reasons, we propose that radical recombination in the formation of the cross-linked Gly₂HisGly species occurs at the α carbons of the N-terminal glycylic residues. First, the proposed site of oxidation at p[H⁺] 8.5–10.3 is similar to the site of oxidation at p[H⁺] 5.4–7.5. The low retention time of species **5** (6.1 min, Figure 4) suggests that the p*K*_a value of at least one of the amino groups is significantly decreased. Cross-linking at the N-terminal glycylic residue, followed by oxidation at this site (Scheme 3), would result in enamino groups with lower the p*K*_a values. Conjugated

enamines exhibit p*K*_a values as low as 2.8.³² Such a p*K*_a change could account for the lower retention time of **5** than **4** on a strong cation-exchange column. Finally, ESI-MS data show that **4** is subject to formylation in the presence of ammonium formate buffer during the chromatographic fraction collection/lyophilization steps, while **5** is not. Amino groups can undergo formylation under these conditions.^{33,34} We propose that the conjugated enamino nitrogens of **5** are significantly less nucleophilic and they are less reactive toward formylation. The n,π conjugation of the amino nitrogen and the C=C double bond draws electron density onto the β carbon.³⁵ As shown in Figure S9, there is no formylation product of the [**5** + H]⁺ adduct at *m/z* 677. However, the mass spectrum of **4** shows a distinct formylation product of the [**4** + H]⁺ adduct at *m/z* 679 (Figure 5).

We propose that this cross-linking occurs between two carbon radicals, although we have also considered the possibilities of C–N or N–N linkages. One-electron oxidations of the N-terminal amine nitrogens and the subsequent recombination of the radicals, followed by oxidation to an azopeptide, are possible. However, azo compounds tend to exhibit absorbances in the visible range (~350 nm),³⁶ and the products observed in this work do not have these spectral characteristics. The possibility of C–N bond formation from carbon and nitrogen radicals, followed by oxidation to an imine, was also considered. However, we have not observed nitrogen atom oxidation in the reactions of Ni(III)– and Cu(III)–peptide complexes.^{5,15–17} For these reasons, we propose that peptide oxidation and radical recombination occur at the α carbon atoms.

Conclusions. This is the first evidence of nickel-mediated formation of cross-linked peptides between two N-terminal glycylic α carbon atoms. Protein–protein cross-linking via Ni(II) and peroxides has been demonstrated, although the cross-linking occurred either between the aromatic side chains of tyrosyl residues^{10,11} or between a tyrosyl side chain and a glycylic α carbon.¹² In this work, the resulting 2,3-diaminobutanedioic acid peptide derivative is readily oxidized by O₂ to give a 2,3-diaminobutenedioic acid peptide derivative. These results are supported by chromatographic and mass spectrometric data. These species are formed via an oxo-bridged Ni(III)–peptide dimer that is supported by kinetic data.³⁰ While the oxo-bridged Ni(III) species in this work is very reactive, a (Ni^{III}salen)₂O species has been isolated and its crystal structure determined.³¹ Our work also represents the first example of a four-electron oxidative self-decomposition by a trivalent metal–peptide complex. Previously, only two-electron oxidations at the peptide have been observed.^{5,15–17}

(32) Leismann, H.; Marzolph, G.; Scharf, H.-D.; Behruzi, M. *Chem. Ber.* **1983**, *116*, 2591–2615.

(33) Viville, R.; Scarso, A.; Durieux, J. P.; Loffet, A. *Pept.: Struct. Funct., Proc. Am. Pept. Symp.*, **8th** **1983**, 747–750.

(34) Reddy, P. G.; Kishore, Kumar G. D.; Baskaran, S. *Tetrahedron Lett.* **2000**, *41*, 9149–9151.

(35) Haeflinger, G.; Mack, H. G. In *The Chemistry of Enamines, Part 1*; Rappoport, Z., Ed.; John Wiley & Sons: New York, 1994; pp 2–3.

(36) Rau, H. *Angew. Chem., Int. Ed. Engl.* **1973**, *12*, 224–235.

Acknowledgment. This work was supported by National Science Foundation Grant CHE-0139876. The authors are grateful for the donation of a lyophilizer by Mary Bower of the Biochemistry Department. The authors also wish to thank Karl V. Wood and Mark A. Lipton for helpful conversations.

Supporting Information Available: Tables of tandem mass spectra, kinetic data, and UV-vis, IR, and EPR spectra. This material is available free of charge via the Internet at <http://pubs.acs.org>.

IC035034X